



UNIVERSIDADE ESTADUAL DE CAMPINAS
SISTEMA DE BIBLIOTECAS DA UNICAMP
REPOSITÓRIO DA PRODUÇÃO CIENTÍFICA E INTELLECTUAL DA UNICAMP

Versão do arquivo anexado / Version of attached file:

Versão do Editor / Published Version

Mais informações no site da editora / Further information on publisher's website:

<https://www.sciencedirect.com/science/article/pii/S0008622313012177>

DOI: 10.1016/j.carbon.2013.12.062

Direitos autorais / Publisher's copyright statement:

©2014 by Elsevier. All rights reserved.

DIRETORIA DE TRATAMENTO DA INFORMAÇÃO

Cidade Universitária Zeferino Vaz Barão Geraldo

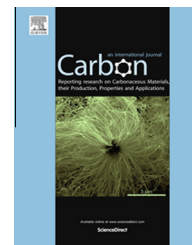
CEP 13083-970 – Campinas SP

Fone: (19) 3521-6493

<http://www.repositorio.unicamp.br>

Available at www.sciencedirect.com

ScienceDirect

journal homepage: www.elsevier.com/locate/carbon

Size-controlled synthesis of graphite nanoflakes and multi-layer graphene by liquid phase exfoliation of natural graphite

A.V. Alaferdov ^{a,b}, A. Gholamipour-Shirazi ^a, M.A. Canesqui ^a, Yu.A. Danilov ^c,
S.A. Moshkalev ^{a,*}

^a Center for Semiconductor Components, State University of Campinas, Campinas, Sao Paulo 13083-870, Brazil

^b Lobachevsky State University of Nizhni Novgorod, Gagarine Av. 32/3, Nizhni Novgorod 603950, Russia

^c Physico-Technical Research Institute of Nizhni Novgorod State University, Gagarine Av. 32/3, Nizhni Novgorod 603950, Russia

ARTICLE INFO

Article history:

Received 24 September 2013

Accepted 22 December 2013

Available online 30 December 2013

ABSTRACT

Multi-layer graphene and graphite nanoflakes were produced through graphite liquid exfoliation using organic solvents. The nanoflakes size distribution was statistically analyzed, with the number of measured samples being high enough (from ~200 to 900) for reliable evaluation of the statistical model. The nanoflakes size data were found to follow a log-normal distribution, with higher fraction of large size flakes as compared to a conventional normal distribution. The same kind of distribution was also obtained for nanoflakes thickness. Based on these findings, the detailed mechanism of the pristine polycrystalline graphite exfoliation in a liquid phase due to formation and collapse of cavitation bubbles was discussed. The high quality of nanoflakes was confirmed by Raman spectroscopy.

© 2013 Elsevier Ltd. All rights reserved.

1. Introduction

Graphene has attracted much interest, owing to its exceptional electrical [1], chemical [2], mechanical [3], and thermal properties [4,5] and numerous potential applications, like batteries [6,7], photovoltaic devices [8], supercapacitors [9], sensors [10], etc. The key factor for many industrial applications is the possibility to deposit and pattern large area graphene sheets in different substrates [11]. Several methods for the graphene synthesis have been reported [12–14], and among them the chemical vapor deposition (CVD) method has been most widely employed to grow large area graphene on metal surfaces that can be further transferred to other substrates [15,16]. However this method is an energy intensive process that might be too expensive for many applications [14,17].

High quality monolayer graphene sheets can also be produced at significant yields by liquid-phase exfoliation of graphite [18–22] and furthermore large amounts of graphene flakes can be used to fabricate large transparent conducting films by different techniques, among them the Langmuir–Blodgett method [11,23,24]. This approach which is simple, low cost, scalable, and versatile in terms of being well-suited to chemical functionalizations, affords the possibility of high-volume production [25], and films derived from liquid suspensions of graphene flakes can potentially overcome the limitations of other methods [26,27] and can be used for a wide range of applications [13].

Graphite can be exfoliated in a non-aqueous ([18,22,23]) or aqueous solutions with a surfactant ([19,28], [29]) with the aid of ultrasound (usually, 20–40 kHz) processing (sonication) which splits the graphite crystallites into individual platelets.

* Corresponding author.

E-mail address: stanisla@ccs.unicamp.br (S.A. Moshkalev).

0008-6223/\$ - see front matter © 2013 Elsevier Ltd. All rights reserved.

<http://dx.doi.org/10.1016/j.carbon.2013.12.062>

With a long time sonication treatment, the fraction of mono-layer or few-layer graphene flakes increases significantly in the suspension, which can be further enriched by centrifugation steps [30]. All these processing steps, as well as the quality of the initial graphite polycrystals determine the quality and the grade of the obtained graphene suspensions [30]. The sonication step has the major effect on the size distribution of the graphene flakes. Two main factors which determine the transformation of materials in this process are cavitation (formation, growth and collapse of highly energetic micro-bubbles [31]) and shear forces. A high-intensity acoustic wave brings about the cavitation, which is a complex non-linear phenomenon leading to concentration of low-density elastic (sound) wave energy into higher densities by rapid bubble collapse at the graphite surface that crushes the bulk material suspended in a liquid. The bubble formation can also occur in the liquid close to the solid (at distances higher than the bubble diameter), in this case energetic micro-jets of solvent that are generated during the bubble collapse, can hit the solid surface with great impact also contributing to the flake delamination. By breaking relatively weak interlayer bonds, the mechanical energy released at the surface of graphite by cavitation removes the top layers leading to delamination and dispersion [29,32]. Due to the anisotropic layered structure of graphite, thin graphene flakes with relatively high aspect ratios (lateral size/thickness) are produced in this process.

There are a few studies where size distributions of graphene flakes (or thin graphite nanoflakes) produced by liquid phase exfoliation of graphite are presented. In most cases, the lateral size and height distributions were evaluated from analyses of electron scanning, electron transmission or atomic force microscopy (SEM, TEM and AFM, respectively) images, with the total number of nanoflakes in measured distributions varying from 60 [28] and 90 [20,33] to ~180 [19]. It should be noted that these numbers are usually not high enough to perform reliable statistical analysis of size distributions that might be helpful for better understanding of the exfoliation mechanisms and further optimization of the process. Different approach was employed by Łoś et al. [29] in a study of graphite exfoliation using ultrasound irradiation at 20 and 500 kHz, where dynamic laser granulometry was applied for analysis of size distributions. In this technique, the particles sizes are determined using the theory of light diffraction by spherical shape particles though real graphene flakes have quite different platelet morphology. This should be taken into account when comparing with other results obtained by direct measurements of lateral dimensions and heights. The lateral sizes of graphene flakes in different studies were reported to vary from 0.2 μm to a few μm [19,20,28,33] or even up to ~200 μm [29], depending on the preparation procedures, and no statistical model has been discussed for obtained size distributions.

In this work, we have analyzed the size distribution of nanoflakes obtained by sonication of natural graphite in two different organic solvents. To obtain reliable data for statistical analysis, large flake numbers (up to 900) were analyzed for each experimental condition studied. The size distributions for nanoflakes were found to follow the log-normal model rather than the conventional normal (Gaussian) one.

The mechanisms responsible for formation of log-normal distributions with extended tails (higher fraction of large size flakes) are discussed. These findings are important for applications where films formed by many flakes are employed. Better understanding of the delamination process, with the help of statistical analysis, is important to produce nanoflakes with desired size range by changing the key process parameters. High quality of obtained flakes was confirmed by high resolution scanning electron and atomic force microscopy, and micro-Raman spectroscopy.

2. Experimental

Natural graphite powder with the average crystal size of 1–3 mm was obtained from Nacional de Grafite, Brazil. Analytical grade 2-propanol (IPA) and *N,N'*-Dimethylformamide (DMF) were obtained from Sigma and used as received.

The graphite was dispersed in the relevant solvent (volume of 1 mL, density of 1 mg/mL) by sonicating in a low power sonic bath (Unique USC-1880, 100 W, 37 kHz). Temperature was kept constant (if not specified, at room temperature, 23 ± 2 °C) during sonication using a home-made coil-shaped heat exchanger immersed into the water bath. The resultant dispersion was then centrifuged using a Mini-Spin Eppendorf AG 22331. After centrifugation, decantation was carried out by pipetting off the top 400 μL of the dispersion, and these samples were used for further analysis. In order to characterize the size distribution of flakes, the obtained suspensions were deposited onto holey amorphous carbon TEM grids (400 mesh) by drop casting. Thin films consisting of graphene flakes were also deposited over thermally oxidized (100) silicon or glass substrates using a drop casting or Langmuir–Blodgett method [11]. Samples with deposited flakes were examined by optical microscopy (Olympus MX51) and high resolution scanning electron microscopy (SEM, Nova 200 Nanolab, FEI). Quality of graphene flakes was analyzed by micro-Raman spectroscopy in confocal configuration (NT-MDT NTEGRA Spectra, with 473 and 633 nm lasers).

3. Results and discussion

Typical example of nanoflakes with different lateral sizes deposited over TEM grids can be seen in Fig. 1. From the analyses of such images, histograms of lateral sizes L for nanoflakes were obtained, with the number of measurements always being high enough (>200, in some cases up to 900) to get reliable statistics. With the aim of validating and comparing the obtained statistical models, the experimental data were fitted by normal and log-normal distributions as well as by two other asymmetric distributions, i.e., of Weibull and Gumbel (Eqs. S1–S4 in Supporting information), which are very similar to the log-normal distribution and are often used to describe these kind of processes [34,35]. Curve fitting was done in the R software version 2.15.1 [36] using the maximum likelihood estimation (MLE) method [36,37]. The results for short and long times of sonication (2 and 240 min) are compared in Fig. 2a and b, respectively. As can be seen, the experimental nanoflake size distribution is described

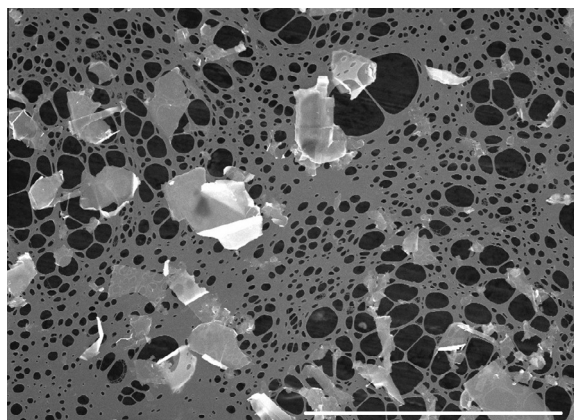


Fig. 1 – SEM image of the graphene flakes deposited from suspension sonicated 240 min in DMF, not centrifuged, scale bar – 20 μm .

better by a log-normal model. The detailed comparison of distributions is presented in [Supporting information \(Table S1\)](#). Note that the log-normal distribution $f_{\text{LN}}(L) = \frac{1}{L\sigma\sqrt{2\pi}} e^{-\frac{1}{2}\left(\frac{\ln(L)-\mu}{\sigma}\right)^2}$ (where L is the size, $f_{\text{LN}}(L)$ is probability

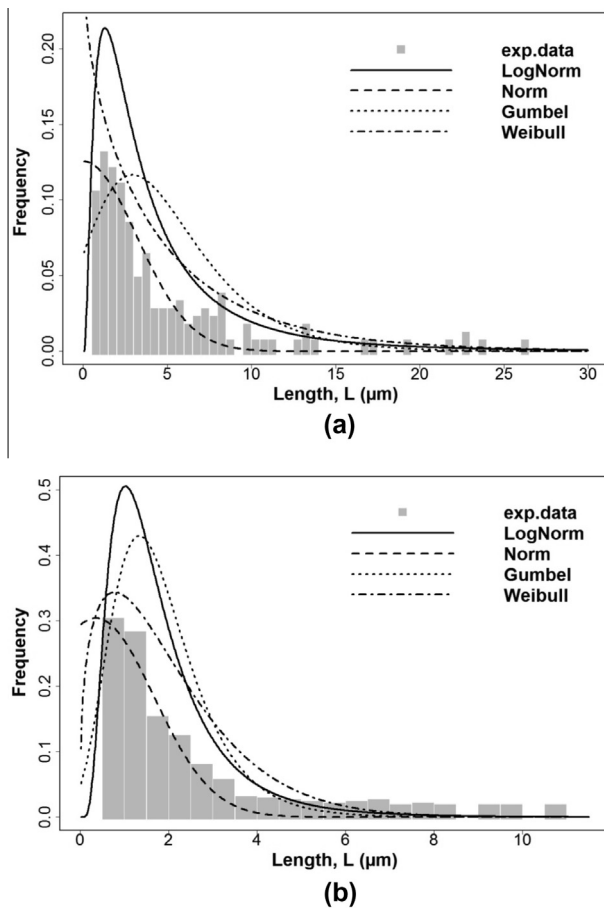


Fig. 2 – A comparison of different distribution models and the experimental data for DMF solvent, plastic vial, no centrifugation: (a) 2 min sonication, total number of flakes – 193 (b) 240 min sonication, total number of flakes – 924.

density function (PDF), μ and σ are parameters of distribution) differs from the more conventional normal or Gaussian distribution $f_G(L) = \frac{1}{\sigma_G\sqrt{2\pi}} e^{-\frac{1}{2}\left(\frac{L-\mu_G}{\sigma_G}\right)^2}$ (μ_G and σ_G are parameters of distribution) basically for large size flakes (the extended distribution tail), and it reproduces much better the experimentally observed elongated tails ([Fig. 2a, b](#)).

The data on size distributions available from other works ([Table 1](#)) employing similar material and methods were treated here with the same methodology, by curve fitting using the MLE method. The analysis was done to show that the log-normal distribution usually can be confirmed for short and medium time sonication treatments (up to 48 h [[20](#)]) and for different solvents or centrifugation parameters. However, long time sonication (e.g., 168 h, [[33](#)]) tends to produce a normal rather than log-normal graphene flakes size distribution (see [Table 1](#), entry c, and [Fig. 3](#)).

The origin of a log-normal flakes size distribution with extended tails can be attributed to the specific mechanisms of graphite exfoliation in liquid phase. Exfoliation of graphite by sonication in a liquid is believed to be the result of sequential random microscopical events like shock waves and micro-jets generated by collapsing cavitation bubbles [[32,38](#)]. Cavitation is known to be a nonlinear phenomenon that concentrates and transforms low-density elastic wave energy into localized higher energy densities through rapid formation and collapse of gas bubbles in the liquid that can occur near or at the graphite surface. The resulting extreme local conditions (effective temperature up to $\sim 5 \times 10^3$ K, the local heating rates within a cavitating bubble $\sim 10^{10}$ – 10^{12} K s $^{-1}$, local pressure ~ 20 – 30 MPa [[31,39](#)]) induce profound changes at the solid–liquid interfaces. Cavitation induced exfoliation can be viewed as an analog of the stochastic multiplicative process of breakage (crushing, bulk attrition) which underlies conventional particle production processes [[35](#)]. It can be shown ([Supporting information](#)) that this kind of Markovian process (when implementation of subsequent states of the object does not depend on its previous state) results in a log-normal size distribution.

The evolution of flakes during the exfoliation process is shown schematically in [Fig. 4](#). For the experimental conditions of the present work (sonication frequency 37 kHz), the size of bubbles is known to range from a few micrometers to ~ 25 μm [[40–42](#)], being thus one or two orders of magnitude smaller than the initial size (~ 1 – 3 mm) of graphite polycrystals. Collapse of the bubble at the flake surface can cause the polycrystal breaking directly by the produced shock waves ([Fig. 4a](#)), whereas collapse in the liquid close to the surface generates a micro-jet of solvent that can hit the solid with a great force [[43](#)]. The pressure required to separate two graphene sheets is estimated to be 7.2 MPa [[44](#)]. The local pressure created by collapsed bubbles (20–30 MPa) [[31,39](#)], is thus sufficient to remove the top layer after disrupting weak molecular interactions, leading to delamination and dispersion of the initial graphite flakes.

It can be expected that polycrystalline natural graphite starts to exfoliate in the areas containing defects and at the grains boundaries ([Fig. 4a](#)). Two stages of the process can be distinguished. First, formation of relatively large submillimeter

Table 1 – Experimental conditions and results obtained in previous reports on graphene synthesis by liquid exfoliation method and their statistical analysis by the methodology of this work.

Entry	Solvent	Initial graphite concentration (mg/mL)	Sonication parameters			Centrifugation parameters		$\langle L \rangle^a$ (μm)	$\langle L \rangle^b$ (μm)	Ref.
			Time (h)	Frequency (kHz)	Power (W)	Time (min)	Rate (rpm)			
a	Water	20	22	20	350	Not centrifuged		33.7	–	[29]
b	Water and surfactant	20	2	20	350	Not centrifuged		16.3	–	[29]
c	N-Methyl-2-pyrrolidone	3.3	168	24	48	45	500	~0.5	0.56	[33] ^d
d	IPA	3.3	48	40	16	45	2000	1.1	1.07	[20]
e	Chloroform	3.3	48	40	16	45	2000	0.84	0.85	[20]
f	Glacial acetic acid with surfactant	10 ^c	4	37	320	45	20,000 (kept overnight)	0.7	0.67	[28]
g	Water with surfactant	0.1	0.5	37	320	90	500 (kept 24 h)	~0.5 ^c	0.33	[19]

^a Data as reported.

^b Data calculated from the reported particle size distribution, using the MLE method.

^c Estimated.

^d Data from the Appendix of the referred paper.

(~0.1 mm) (Fig. 4b) primary flakes from the initial millimeter-size graphite crystals (marked as a “delta-function” in Fig. 4a) is likely to occur. Further, as a result of subsequent cavitation and delamination events, the primary flakes are sequentially exfoliated to form secondary micrometer-size nanoflakes. In other words, the initial delta-function-like distribution gradually spreads and transforms into a log-normal distribution with the center of the distribution still located in the large size flakes area (Fig. 4c). During the initial phase of the exfoliation, the delamination sequentially removes top surface layers of natural graphite flakes and thus reduces slowly the dimensions of “mother” flakes. Note that the lifetime (time during which the flake retains its size) for large primary flakes (“mothers” flakes) is much larger than for smaller flakes. As the process goes further, the center of distribution shifts to smaller size flakes and therefore micrometer-size flakes start to gain weight in the distribution (Fig. 4d) (see also [29]). More flakes with a few micron size form for longer sonication times. Lateral size of flakes formed at this stage is not more than the mean cavitation bubble size (see Fig. 4e), note that similar distribu-

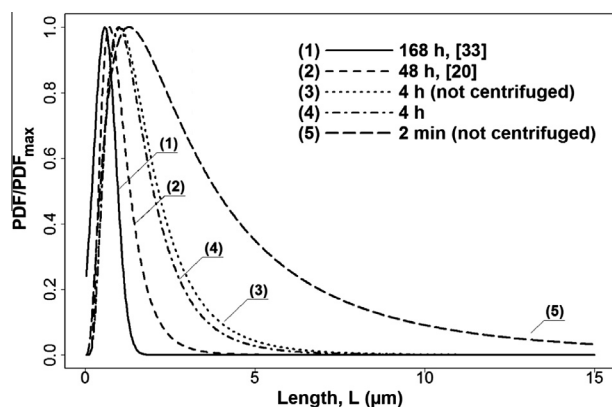


Fig. 3 – Graphene flakes size distribution for different times of sonication treatment (normalized probability density function or PDF), data from the present study (Table 2) and adapted from Refs. [20,33].

tions can be found in Ref. [20]. As time goes to “infinity”, distribution of lateral size of graphene turns into normal (Gaussian) distribution with the center at the origin of coordinates (Fig. 4f), see also [33]. At this stage, it is likely that the mean size of nanoflakes is comparable with that of the bubbles, so that new flakes formation becomes difficult, and breaking the new flakes is no more a Markovian process (as it was during the initial stage of delamination). In other words, splitting (delamination) of the subsequent secondary flakes becomes dependent on the size of the primary flake. In the present work, graphene nanoflakes size distribution was found to be still close to the log-normal distribution even after 240 min of sonication (Fig. 2b), whereas the distribution very close to normal was indeed observed for sonication time as long as 168 h [33] (Fig. 3).

Several experiments were carried out in order to investigate the effect of various synthesis parameters such as solvent type, the duration of sonication and centrifugation as well as the vial material. Experimental data were fitted by a log-normal distribution also using MLE methods. The effect of the sonication time on graphene flakes size distribution is demonstrated in Table 2 and Fig. 5.

The mean size of flakes (Table 2) is decreased considerably with increasing sonication time: from 4.80 to 1.86 μm (2 and 240 min of sonication, no centrifugation) and from 1.98 to 1.45 μm (2 and 60 min. sonication, 15 min. centrifugation). The effect seems to be more pronounced without the centrifugation step.

After 240 min. of sonication, most of all flakes were in the range of (0.8, 2.9) μm (Fig. 5 and Table S2, Supporting information). Flakes larger than 5 μm were rarely observed, in contrast to 2 min. of sonication when flakes with size up to 50 μm were present.

The data (Table 2) also suggest that the mean size of nanoflakes scales with sonication time as t^{-n} , where $n \sim 0.2$ (slowly reduces with the sonication time), that correlates well with other studies where similar trend was reported (Table 1, entries c, d, e) [19,20,32].

The effect of centrifugation on the distribution was found to be very strong, especially for short sonication times. For sonication time of 2 min., even after a mild centrifugation

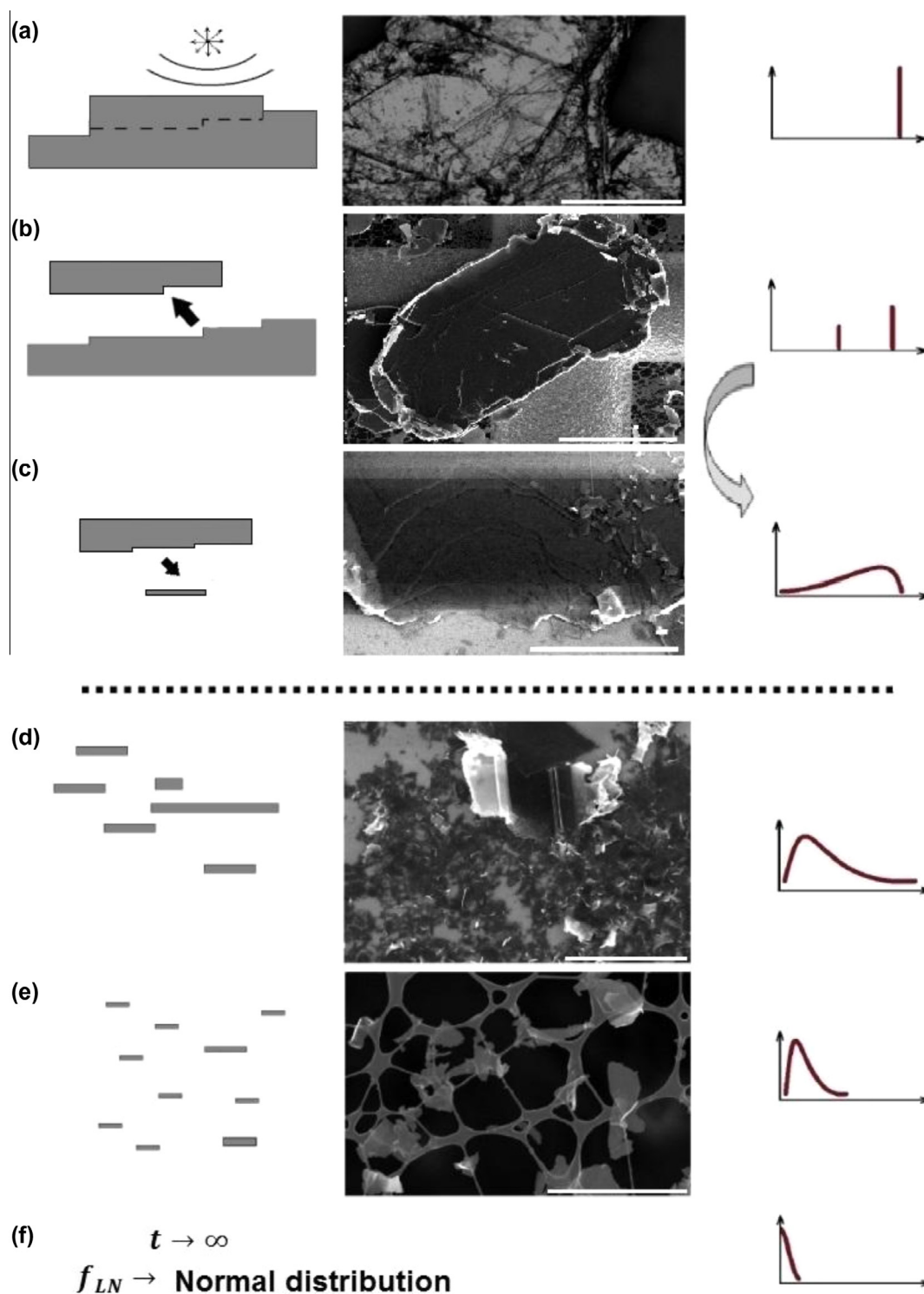


Fig. 4 – The schematic of the exfoliation process. Images: (a) fragment of the initial graphite crystal, (b) large primary flake, (c) result of delamination from the primary leaving a staircase-like surface, (d) large number of small secondary flakes, (e) small flakes captured by the TEM grid. Scale bars: (a) –300 μm , (b) –25 μm , (c) 10 μm , (d) –10 μm , (e) 4 μm . Note that the TEM grid can capture flakes smaller than the size of holes in the grid (as can be seen in e), however large fraction of smaller flakes can be washed out through the holes, resulting in fast fall of the experimental distribution probability near the origin of coordinates. (A colour version of this figure can be viewed online.)

(15 min, 800 rpm), proportion of large flakes with $L > 6.5 \mu\text{m}$ decreased dramatically to less than 1%, whereas the not centrifuged suspension contains around 15% of large flakes

($L > 11 \mu\text{m}$) (Fig. 5, curves 1 and 3, Table S3 in Supporting Information). This means that large flakes and aggregates ($L > 10 \mu\text{m}$) are completely removed by mild centrifugation,

Table 2 – Effect of sonication and centrifugation time on the size of graphene flakes prepared in glass vials for IPA and in plastic vials using DMF as solvent, centrifuged at 800 rpm. $\langle L \rangle$ mean size of graphene flake.

Solvent	Sonication time (min)	Centrifugation time (min)	$\langle L \rangle$ (μm)
DMF	2	0 (not centrifuged)	4.8
	240	0 (not centrifuged)	1.9
	2	15	2.0
	60	15	1.5
	240	15	1.7
IPA	60	90	1.8
	60	15	1.1
	60	60	1.1

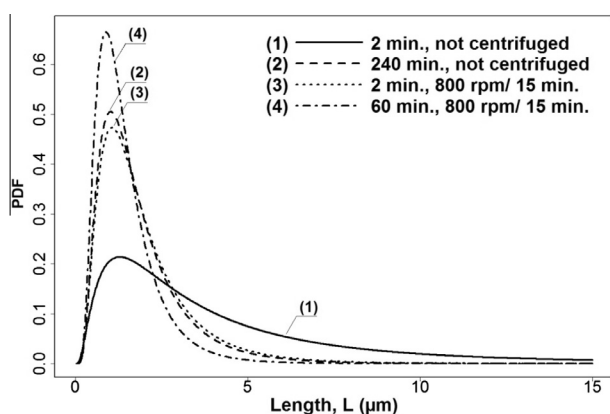


Fig. 5 – Probability distribution for graphene flakes lateral size, as function of sonication time. Graphene flakes prepared in plastic vial in DMF as solvent: (1) and (2) at 2 and 240 min respectively without centrifugation; (3) and (4) at 2 and 60 min respectively, after centrifugation at 800 rpm for 15 min. The number of flakes is (1) 193, (2) 924, (3) 333 and (4) 427.

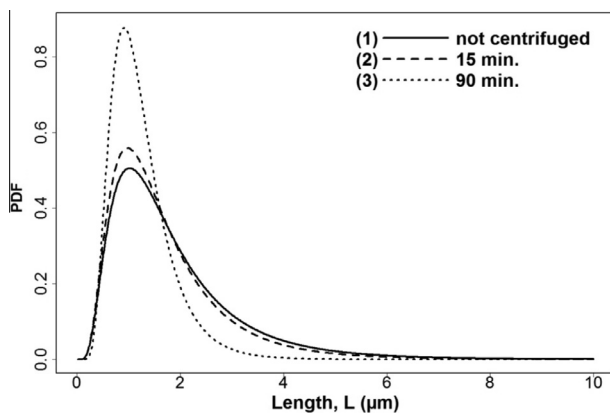


Fig. 6 – Probability distribution for nanoflakes lateral dimension to investigate the effect of centrifugation time at prolonged sonication treatment. Nanoflakes prepared in plastic vials and DMF as solvent, after 240 min of sonication treatment (1) – not centrifuged, (2) and (3) centrifuged at 15 and min. respectively. The number of flakes is (1) 924, (2) 578 and (3) 193.

giving a relatively homogeneous dark gray dispersion. Although some sedimentation and aggregation was observed to occur within the first week after centrifugation, the obtained dispersions remained stable for at least 4 months after preparation.

For samples with a prolonged sonication treatment of 240 min. (Fig. 6), practically no changes in graphene size distribution were observed after 15 min. of centrifugation (compare curves 1 and 2 in Fig. 6). However, after increasing the centrifugation time up to 90 min., the flakes with sizes exceeding $L > 4 \mu\text{m}$ were totally removed, and 97% of flakes have sizes smaller than $2.8 \mu\text{m}$ (proportions of flakes with $0.7 < L < 2.8$ and smaller flakes with $0.3 < L < 0.7$ are $\sim 82\%$ and $\sim 15\%$, respectively), with $\langle L \rangle = 1.2 \mu\text{m}$. Therefore, centrifugation time of 90 min at 800 rpm can be used for selecting flakes with sizes within the range of $1\text{--}4 \mu\text{m}$.

During sonication over a prolonged period, the sonication bath water tends to heat up to around 40°C without cooling for temperature moderation (see Section 2 for details). However, we found that the heat generated during sonication had no significant effect on graphene flakes size (Table S4 and Fig. 1S in Supporting information).

Regarding the effect of solvents on the size distribution, it has already been shown that the enthalpy of mixing for graphite dispersed in good solvents is very close to zero, and the solvent–graphite interaction is van der Waals rather than covalent [18]. Moreover, good solvents for graphene are usually characterized by surface tensions in the range of $40\text{--}50 \text{ mJ m}^{-2}$ (surface energy of graphene at room temperature is 46.7 mJ m^{-2} [45]) with a Hildebrand solubility parameter (δ_T) close to that of graphene ($23 \text{ MPa}^{1/2}$) [46]. Values of δ_T for the solvents used here are very close to that of graphene: 24.9 and $23.6 \text{ MPa}^{1/2}$ for DMF and IPA, respectively (Table S7 in Supporting information). Very similar behavior, with respect to graphite exfoliation was found for the two solvents, with graphene size distributions characterized by practically the same mean size and width (Fig. S2 and Table S5 in Supporting information). However, in case of IPA the sedimentation was found to be faster, probably due to its lower surface energy. Hernandez et al. [18] have shown that effective solvents for graphene have surface tensions close to 40 mJ m^{-2} . The surface tension of DMF (37.1 mJ m^{-2}) is closer to that of graphene than surface tension of IPA (23 mJ m^{-2}) which in turn could result in slower sedimentation in DMF (Fig. 7).

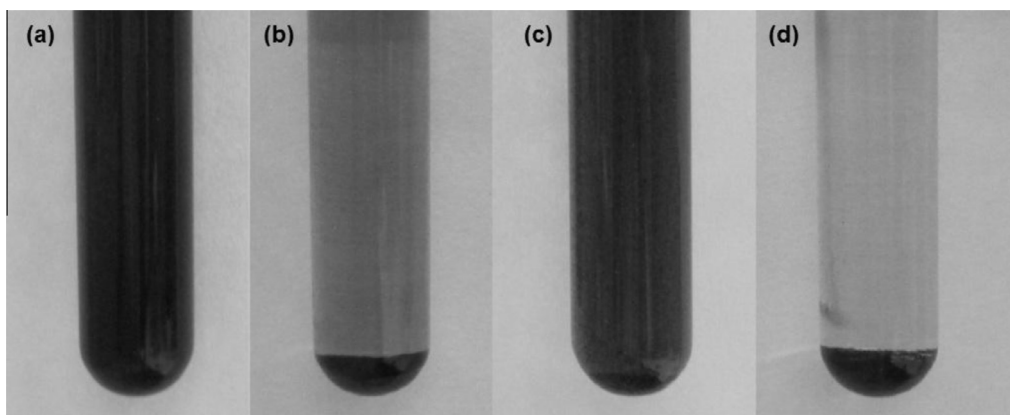


Fig. 7 – Sedimentation study. Suspensions of graphene prepared at concentration of 1 mg mL^{-1} and sonicated 120 min. in a glass vial without further centrifugation. (a) Solvent DMF, (b) sample(a) after 75 days, (c) solvent IPA, (d) sample (b) after 75 days.

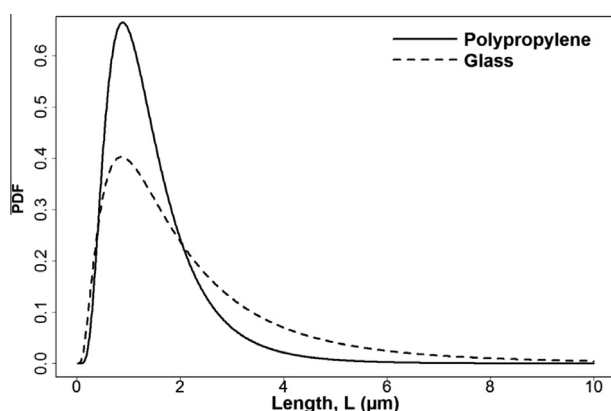


Fig. 8 – Probability distribution for nanoflakes lateral dimension to investigate the effect of vial material on the size of flakes prepared in DMF, sonicated for 60 min and centrifuged at 800 rpm for 15 min at room temperature.

Both plastic (polypropylene) and glass vials were utilized in experiments. Polypropylene is resistant to IPA and to DMF up to 60°C . However, ultrasound energy can be absorbed strongly in plastics resulting in less intense ultrasound processing of graphite. Surprisingly, we observed that the graphene flakes are larger in glass vials (Fig. 8 and Table S6 in Supporting information), under similar processing conditions (60 min. sonication, centrifugation at 800 rpm for 15 min.). We attribute this effect to stronger production of large primary flakes in glass vials that are not completely removed by centrifugation, as the time of sonication (60 min.) is not enough to completely break and delaminate the large size flakes. Note that for longer sonication time, when large flakes are completely broken (this will happen faster for glass vials where the density of ultrasound energy in the solution is higher), more compact distribution for glass rather than for plastics vials can be expected, in contrast to that shown in Fig. 8.

The crystalline quality of nanoflakes deposited over TEM grids was evaluated using confocal Raman spectroscopy. Representative Raman spectra (at least, 5 spectra were taken for each sample) are shown in Fig. 9, where a low intensity

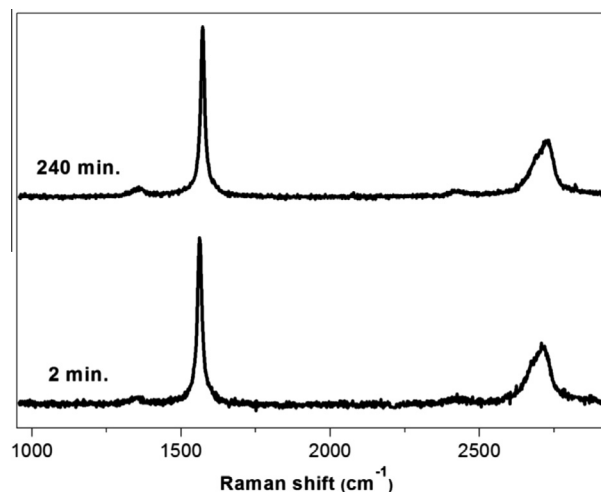


Fig. 9 – Raman spectra for samples sonicated for 2 and 240 min and centrifuged at 800 rpm for 15 min (Table 2).

D-band ($\sim 1345 \text{ cm}^{-1}$), strong G-band ($\sim 1570 \text{ cm}^{-1}$) and a moderately intense 2D band ($\sim 2700 \text{ cm}^{-1}$) can be seen. The defect content in graphene layers is usually characterized by the ratio of intensities for D and G bands (I_D/I_G) [12,47]. From the measured I_D/I_G ratio, the in-plane crystallite size L_a can be estimated [48]. It is observed that the ratio is practically the same for both processes, being at a very low level $I_D/I_G \sim 0.10$ ($L_a \sim 0.12 \mu\text{m}$) compared with other studies (Table 3) for flakes after 2 and 240 min. of sonication. We obtained even lower values ($I_D/I_G < 0.05$) for large number of flakes [49]. This indicates that for sonication time up to 240 min. almost defect-free flakes are obtained and no additional defects are added [50]. As can be expected, high values of I_D/I_G are observed for experiments carried out in water and mixture of water and surfactant [28] (Table 3). A high value of I_D/I_G has been reported with NMP as a solvent, despite being a good solvent for graphite liquid exfoliation ($\delta_T = 23 \text{ MPa}^{1/2}$ [46], i.e., matching perfectly with that of graphene (Table 3), probably due to a very long sonication time (168 h).

Note that alternative graphene synthesis methods are usually characterized by higher values of I_D/I_G . For example,

Table 3 – Reported values of I_D/I_G -against time of sonication and type of solvent.

Solvent	Time of sonication (h)	I_D/I_G	Ref.
Water	22	0.6	[29]
Water/surfactant	2	0.6	[29]
N-Methyl-2-pyrrolidone	168	0.2	[33]
IPA	48	0.2–0.7 ^a	[20]

^a Depending to the flake size.

Chabot et al. [51] have reported a value of 0.25 for the process where graphene was obtained by Gum Arabic assisted physical sonication, while Reina et al. [26] and Cheng et al. [52] have reported $I_D/I_G = 0.93$ and $I_D/I_G = 0.05$ – 0.3 respectively using chemical vapor deposition of graphene. Different electrochemical methods for graphene synthesis give an I_D/I_G value in the range of 0.1–0.6 [53]. Here, a combination of a suitable solvent selection as well as relatively short

sonication time provides almost a defect-free nanographite and multi-layer graphene product. The high quality of nanoflakes is also confirmed by observations of very narrow G-lines in Raman spectra. The full width at half maximum (FWHM) for G lines was found to vary within 18–21 cm^{-1} at short sonication time (2 min.) and was as low as 12–16 cm^{-1} at 240 min. sonication. The reduction of the FWHM for longer processing time probably indicates improved quality (less defects) of obtained flakes. It is also noteworthy that, according to Raman and AFM measurements, FWHM tends to be around 12–14 cm^{-1} for thin flakes (3–15 nm) and 19–21 cm^{-1} for thicker flakes (more than 20 nm).

Thickness of nanosheets deposited on oxidized Si substrates by the Langmuir–Blodgett method, was obtained by atomic force microscopy (AFM). The data were treated with the same methodology described above. Interestingly, a log-normal distribution with an extended tail was also observed for the thickness probability distribution (Fig. 10b). The AFM data show that in the experiment conducted with 4 h of sonication and after 7 days of sedimentation, the major part of

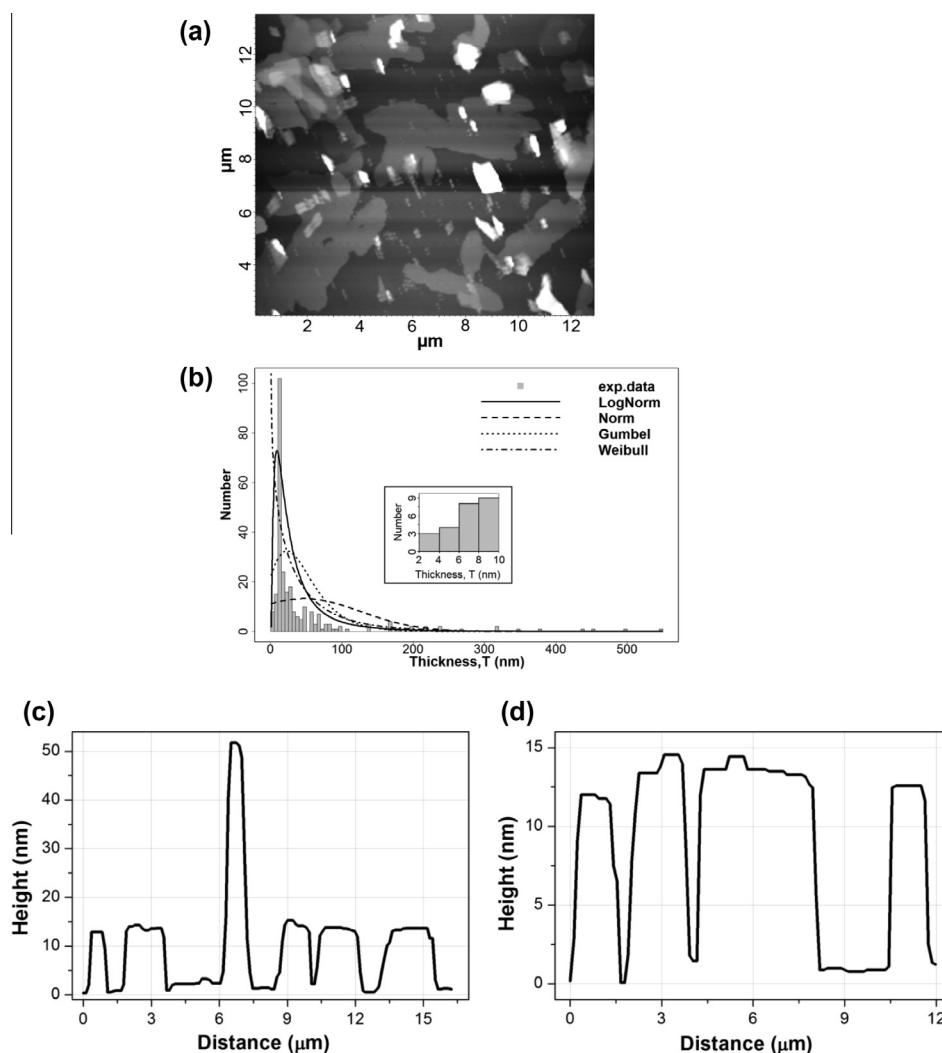


Fig. 10 – (a) AFM-image of nanoflakes deposited on oxidized Si substrates by Langmuir Blodgett method, (b) probability distribution of thickness for nanoflakes, inset: distribution for small size flakes. (c), (d) AFM height profiles of nanoflakes film on Si substrate at two different positions.

flakes (~68%) has a thickness within the range of 9–66 nm, whereas fractions of very thick (>180 nm) or very thin (<3.3 nm) ones (i.e., multi-layer graphene) are less than 2%. It is noteworthy that the thickness of most of flakes is around 11–14 nm (see examples of AFM height profiles in Fig. 10c and d). It might indicate that nanographite monocrystals with the characteristic thickness near 10–12 nm exist in natural graphite, that are delaminated from the larger polycrystalline graphite flakes under impact of collapsing bubbles.

Surfactant-free dispersions can also be used for deposition of individual nanoflakes between the metal electrodes (Au, Ti, W) with micron-scale gaps by a dielectrophoresis method (Fig. 11), similarly to nanotubes [54–56]. This allows us to measure the electrical and thermal contact resistivities between graphene surface and different metals [49,57]. Furthermore, thermal properties of suspended flakes were studied using micro-Raman spectroscopy. The thermal conductivity (near room temperature) for nanoflakes with lateral dimensions less than 1 μm was measured to be $\sim 600 \text{ W m}^{-1} \text{ K}^{-1}$ [49]. This value is quite close to the highest reported values for small nanoflakes [5,49,58,59], proving thus their high crystalline quality that is important for applications in a form of thin continuous films for example in thermal interface materials [58,59].

In another application, the graphene flake suspensions were used to deposit continuous thin films of flakes over various substrates (glass and thermally oxidized Si) using the Langmuir–Blodgett method. For this, a DMF solution with nanoflakes was mildly centrifuged at first to remove large aggregates. Then the supernatant was centrifuged again at

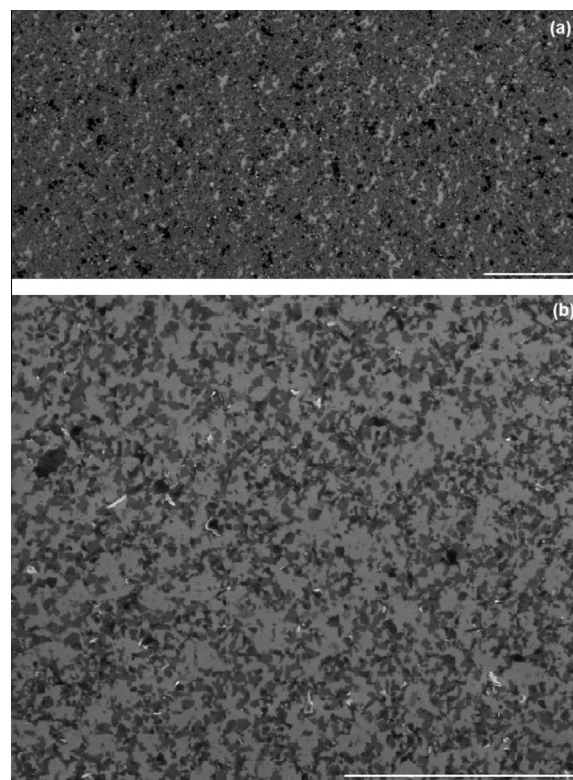


Fig. 12 – Langmuir–Blodgett films of nanoflakes deposited onto Si/SiO₂ substrates: (a) optical image, (b) SEM image. Scale bar; (a) 500 μm , (b) 20 μm .

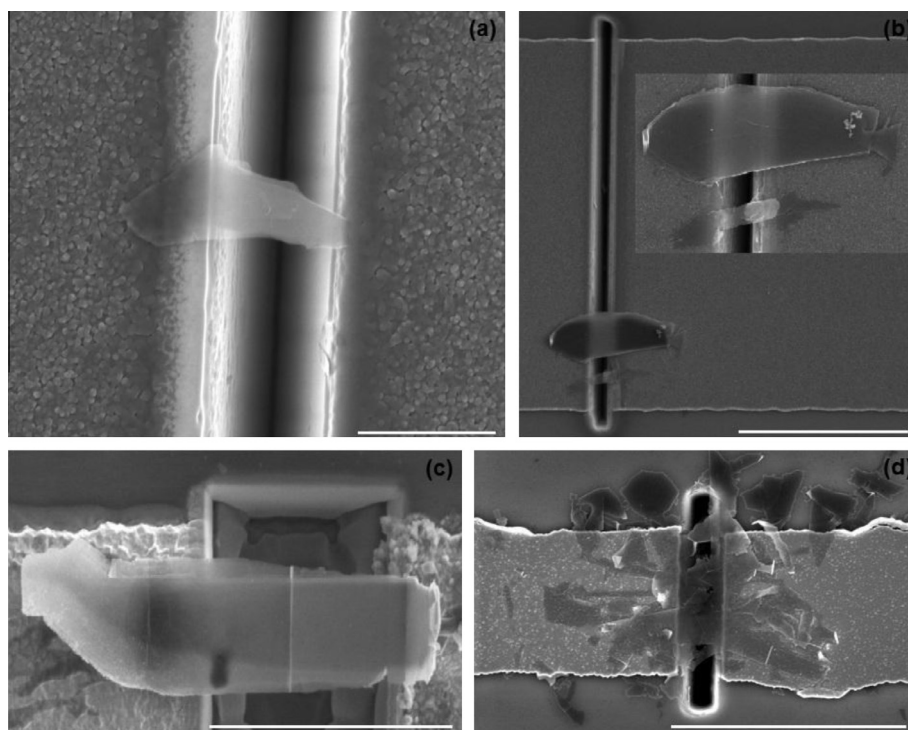


Fig. 11 – Graphene flakes deposited between different metal electrodes with different deposition bias and time (a) Ti, 0.5 V and 30 s. Scale bar: 1 μm ; (b) Ti, 0.5 V and 60 s. Scale bar: 10 μm ; (c) Au, 1.3 V and 30 s. Scale bar: 10 μm ; (d) W, 1.5 V and 90 s. Scale bar: 5 μm .

10,000 rpm for 10 min and the sediment was later transferred to another solvent (toluene or dichloromethane). High surface coverage by nanoflakes with the mean film thickness between 10 and 30 nm was obtained (Fig. 12). The detailed method and comprehensive optimized results including deposition of continuous films will be reported elsewhere [60].

4. Conclusions

In conclusion, graphite nanoflakes and multi-layer graphene flakes were produced by mild sonication in organic solvents (DMF, IPA) and the flakes size distribution was statistically analyzed, with the number of measured samples being high enough (from ~200 to 900) for reliable evaluation of the statistics model. This study has shown that the lateral size data for nanoflakes are better described by a log-normal distribution, with higher fraction of large size flakes as compared to a conventional normal distribution. The same kind of distribution was also obtained for the nanoflakes thickness. Based on these findings, the detailed mechanism of the polycrystalline graphite exfoliation in a liquid phase due to formation and collapse of cavitation bubbles is discussed. We found that for the solvent type, sonication time (from 2 to 240 min.) and process temperature (15–40 °C), as well as centrifugation parameters, within the conditions of our experiments, do not change the type of size distribution that remains log-normal. However, sonication and centrifugation times have notable effect on the mean flakes size; prolonged processes lead to reduced fraction of larger flakes. Better understanding of the delamination process due to impact by collapsing bubbles and resulting shock waves and liquid micro-jets is important to synthesize nanoflakes within the desired size range by changing key process parameters.

By selecting a suitable organic solvent (with the Hildebrand solubility parameter and surface energy close to that of graphene) and other process parameters to provide mild delamination, we demonstrated that high quality (defect free) nanoflakes can be obtained. The quality of flakes has been characterized by confocal Raman spectroscopy. The obtained dispersions were successfully used to deposit flakes between metal electrodes by dielectrophoresis and over various surfaces using Langmuir–Blodgett method, thus demonstrating applicability of dispersions to fabricate both discrete devices and thin continuous films based on high-quality nanoflakes obtained in a low cost process.

Acknowledgments

The authors acknowledge financial support from CNPq, FAPESP and INCT NAMITEC, (Brazil), Dr. Alfredo Vaz for his technical assistance in SEM imaging and in dielectrophoresis deposition experiments and Dr Victor Ermakov for his assistance in R programming.

Appendix A. Supplementary data

Supplementary data associated with this article can be found, in the online version, at <http://dx.doi.org/10.1016/j.carbon.2013.12.062>.

REFERENCES

- [1] Novoselov KS, Geim AK, Morozov SV, Jiang D, Zhang Y, Dubonos SV, et al. Electric field effect in atomically thin carbon films. *Science* 2004;306:666–9.
- [2] Elias DC, Nair RR, Mohiuddin TMG, Morozov SV, Blake P, Halsall MP, et al. Control of graphene's properties by reversible hydrogenation: evidence for graphane. *Science* 2009;323:610–3.
- [3] Stankovich S, Dikin DA, Dommett GHB, Kohlhaas KM, Zimney EJ, Stach EA, et al. Graphene-based composite materials. *Nature* 2006;442:282–6.
- [4] Balandin AA, Ghosh S, Bao W, Calizo I, Teweldebrhan D, Miao F, et al. Superior thermal conductivity of single-layer graphene. *Nano Lett* 2008;8:902–7.
- [5] Balandin AA. Thermal properties of graphene and nanostructured carbon materials. *Nat Mater* 2011;10:569–81.
- [6] Yoo E, Kim J, Hosono E, Zhou H, Kudo T, Honma I. Large reversible Li storage of graphene nanosheet families for use in rechargeable lithium ion batteries. *Nano Lett* 2008;8:2277–82.
- [7] Wang G, Shen X, Yao J, Park J. Graphene nanosheets for enhanced lithium storage in lithium ion batteries. *Carbon* 2009;47:2049–53.
- [8] Liu Z, Liu Q, Huang Y, Ma Y, Yin S, Zhang X, et al. Organic photovoltaic devices based on a novel acceptor material: graphene. *Adv Mater* 2008;20:3924–30.
- [9] Stoller MD, Park S, Zhu Y, An J, Ruoff RS. Graphene-based ultracapacitors. *Nano Lett* 2008;8:3498–502.
- [10] Yang W, Ratinac KR, Ringer SP, Thordarson P, Gooding JJ, Braet F. Carbon nanomaterials in biosensors: should you use nanotubes or graphene? *Angewandte Chemie* 2010;49:2114–38 [International Ed in English].
- [11] Zheng Q, Ip WH, Lin X, Yousefi N, Yeung KK, Li Z, et al. Transparent conductive films consisting of ultralarge graphene sheets produced by Langmuir–Blodgett assembly. *ACS Nano* 2011;5:6039–51.
- [12] Rao CNR, Sood AK, Subrahmanyam KS, Govindaraj A. Graphene: the new two-dimensional nanomaterial. *Angewandte Chemie* 2009;48:7752–77 [International Ed in English].
- [13] Park S, Ruoff RS. Chemical methods for the production of graphenes. *Nat Nanotechnol* 2009;4:217–24.
- [14] Soldano C, Mahmood A, Dujardin E. Production, properties and potential of graphene. *Carbon* 2010;48:2127–50.
- [15] Li X, Cai W, An J, Kim S, Nah J, Yang D, et al. Large-area synthesis of high-quality and uniform graphene films on copper foils. *Science* 2009;324:1312–4 [New York, NY].
- [16] Kim KS, Zhao Y, Jang H, Lee SY, Kim JM, Kim KS, et al. Large-scale pattern growth of graphene films for stretchable transparent electrodes. *Nature* 2009;457:706–10.
- [17] Oyer AJ, Carrillo J-MY, Hire CC, Schniepp HC, Asandei AD, Dobrynin AV, et al. Stabilization of graphene sheets by a structured benzene/hexafluorobenzene mixed solvent. *J Am Chem Soc* 2012;134:5018–21.
- [18] Hernandez Y, Nicolosi V, Lotya M, Blighe FM, Sun Z, De S, et al. High-yield production of graphene by liquid-phase exfoliation of graphite. *Nat Nanotechnol* 2008;3:563–8.
- [19] Lotya M, Hernandez Y, King PJ, Smith RJ, Nicolosi V, Karlsson LS, et al. Liquid phase production of graphene by exfoliation of graphite in surfactant/water solutions. *J Am Chem Soc* 2009;131:3611–20.
- [20] O'Neill A, Khan U, Nirmalraj PN, Boland J, Coleman JN. Graphene dispersion and exfoliation in low boiling point solvents. *J Phys Chem C* 2011;115:5422–8.

- [21] Khan U, O'Neill A, Lotya M, De S, Coleman JN. High-concentration solvent exfoliation of graphene. *Small* 2010;6:864–71 [Weinheim an Der Bergstrasse, Germany].
- [22] Wang X, Fulvio PF, Baker GA, Veith GM, Unocic RR, Mahurin SM, et al. Direct exfoliation of natural graphite into micrometre size few layers graphene sheets using ionic liquids. *Chem Commun* 2010;46:4487–9 [Cambridge, England].
- [23] Li X, Zhang G, Bai X, Sun X, Wang X, Wang E, et al. Highly conducting graphene sheets and Langmuir–Blodgett films. *Nat Nanotechnol* 2008;3:538–42.
- [24] Cote LJ, Kim F, Huang J. Langmuir–Blodgett assembly of graphite oxide single layers. *J Am Chem Soc* 2009;131:1043–9.
- [25] Coleman JN. Liquid exfoliation of defect-free graphene. *Acc Chem Res* 2013;46:14–22.
- [26] Reina A, Jia X, Ho J, Nezich D, Son H, Bulovic V, et al. Large area, few-layer graphene films on arbitrary substrates by chemical vapor deposition. *Nano Lett* 2009;9:30–5.
- [27] Avouris P, Dimitrakopoulos C. Graphene: synthesis and applications. *Mater Today* 2012;15:86–97.
- [28] Vadukumpully S, Paul J, Valiyaveetil S. Cationic surfactant mediated exfoliation of graphite into graphene flakes. *Carbon* 2009;47:3288–94.
- [29] Łoś S, Duclaux L, Alvarez L, Hawelek Ł, Duber S, Kempniński W. Cleavage and size reduction of graphite crystal using ultrasound radiation. *Carbon* 2013;55:53–61.
- [30] Novoselov KS, Fal'ko VI, Colombo L, Gellert PR, Schwab MG, Kim K. A roadmap for graphene. *Nature* 2012;490:192–200.
- [31] Suslick KS, Flannigan DJ. Inside a collapsing bubble: sonoluminescence and the conditions during cavitation. *Annu Rev Phys Chem* 2008;59:659–83.
- [32] Cravotto G, Cintas P. Sonication-assisted fabrication and post-synthetic modifications of graphene-like materials. *Chemistry* 2010;16:5246–59 [Weinheim an Der Bergstrasse, Germany].
- [33] Khan U, O'Neill A, Porwal H, May P, Nawaz K, Coleman JN. Size selection of dispersed, exfoliated graphene flakes by controlled centrifugation. *Carbon* 2012;50:470–5.
- [34] Alves MIF, Neves C. International encyclopedia of statistical science. Berlin, Heidelberg: Springer; 2011.
- [35] Fieller NRJ, Flenley EC, Olbricht W. Statistics of particle size data. *Appl Stat* 1992;41:127–46.
- [36] R: A language and environment for statistical computing. R Foundation for statistical computing; 2008.
- [37] Venables WN, Ripley BD. Modern applied statistics with S. New York, NY: Springer; 2002.
- [38] Skrabalak SE. Ultrasound-assisted synthesis of carbon materials. *Phys Chem Chem Phys* PCCP 2009;11:4930–42.
- [39] Krishnamoorthy K, Kim G-S, Kim SJ. Graphene nanosheets: ultrasound assisted synthesis and characterization. *Ultrason Sonochem* 2013;20:644–9.
- [40] Mettin R, Luther S, Ohl C-D, Lauterborn W. Acoustic cavitation structures and simulations by a particle model. *Ultrason Sonochem* 1999;6:25–9.
- [41] Burdin F, Tsochatzidis NA, Guiraud P, Wilhelm AM, Delmas H. Characterisation of the acoustic cavitation cloud by two laser techniques. *Ultrason Sonochem* 1999;6:43–51.
- [42] Brotchie A, Grieser F, Ashokkumar M. Effect of power and frequency on bubble-size distributions in acoustic cavitation. *Phys Rev Lett* 2009;102:084302.
- [43] Mason TJ, Cintas P. Handbook of green chemistry and technology. Blackwell Science; 2002.
- [44] Jang BZ, Zhamu A. Processing of nanographene platelets (NGPs) and NGP nanocomposites: a review. *J Mater Sci* 2008;43:5092–101.
- [45] Wang S, Zhang Y, Abidi N, Cabrales L. Wettability and surface free energy of graphene films. *Langmuir ACS J Surf Colloids* 2009;25:11078–81.
- [46] Hernandez Y, Lotya M, Rickard D, Bergin SD, Coleman JN. Measurement of multicomponent solubility parameters for graphene facilitates solvent discovery. *Langmuir ACS J Surf Colloids* 2010;26:3208–13.
- [47] Pimenta MA, Dresselhaus G, Dresselhaus MS, Cançado LG, Jorio A, Saito R. Studying disorder in graphite-based systems by Raman spectroscopy. *Phys Chem Chem Phys* PCCP 2007;9:1276–91.
- [48] Cançado LG, Takai K, Enoki T, Endo M, Kim YA, Mizusaki H, et al. Measuring the degree of stacking order in graphite by Raman spectroscopy. *Carbon* 2008;46:272–5.
- [49] Ermakov VA, Alaferdov AV, Vaz AR, Baranov AV, Moshkalev SA. Nonlocal laser annealing to improve thermal contacts between multi-layer graphene and metals. *Nanotechnology* 2013;24:155301.
- [50] Janowska I, Vigneron F, Bégin D, Ersen O, Bernhardt P, Romero T, et al. Mechanical thinning to make few-layer graphene from pencil lead. *Carbon* 2012;50:3106–10.
- [51] Chabot V, Kim B, Sloper B, Tzoganakis C, Yu A. High yield production and purification of few layer graphene by gum arabic assisted physical sonication. *Sci Rep* 2013;3:1378.
- [52] Cheng IF, Xie Y, Allen Gonzales R, Brejna PR, Sundararajan JP, Fouetio Kengne BA, et al. Synthesis of graphene paper from pyrolyzed asphalt. *Carbon* 2011;49:2852–61.
- [53] Low CTJ, Walsh FC, Chakrabarti MH, Hashim MA, Hussain MA. Electrochemical approaches to the production of graphene flakes and their potential applications. *Carbon* 2013;54:1–21.
- [54] Gelamo RV, Rouxinol FP, Verissimo C, Vaz AR, Bica de Moraes MA, Moshkalev SA. Low-temperature gas and pressure sensor based on multi-wall carbon nanotubes decorated with Ti nanoparticles. *Chem Phys Lett* 2009;482:302–6.
- [55] León J, Flacker A, Vaz AR, Verissimo C, De Moraes MB, Moshkalev SA. Electrical characterization of multi-walled carbon nanotubes. *J Nanosci Nanotechnol* 2010;10:6234–9.
- [56] Alaferdov AV, Savu R, Canesqui MA, Vaz AR, Ermakov VA, Moshkalev SA. Study of the thermal contact between carbon nanotubes and a metal electrode. *J Surf Invest X-ray Synchrotron Neutron Tech* 2013;7:607–11.
- [57] Rouxinol FP, Gelamo RVRV, Amici RG, Vaz AR, Moshkalev SA. Low contact resistivity and strain in suspended multilayer graphene. *Appl Phys Lett* 2010;97:253104.
- [58] Goyal V, Balandin AA. Thermal properties of the hybrid graphene-metal nano-micro-composites: applications in thermal interface materials. *Appl Phys Lett* 2012;100:073113.
- [59] Shahil KMF, Balandin AA. Graphene-multilayer graphene nanocomposites as highly efficient thermal interface materials. *Nano Lett* 2012;12:861–7.
- [60] Alaferdov AV, Gholamipour-Shirazi A, Canesqui MA, Moshkalev SA. Fabrication of a chemical sensor based on multilayer graphene/quantum dots using Langmuir–Blodgett method. [Unpublished Work] 2014.